Ionic strength controls long-term cell-surface interactions – A QCM-D study of *S. cerevisiae* adhesion, retention and detachment

Derick Yongabi [a*], Stijn Jooken [a], Stella Givanoudi [a], Mehran Khorshid [a], Olivier Deschaume[a], Carmen Bartic[a], Patricia Losada-Pérez[b], Michael Wübbenhorst [a], Patrick Wagner [a]

[a] KU Leuven, Department of Physics and Astronomy, Laboratory for Soft Matter and Biophysics, Celestijnenlaan 200 D, B-3001 Leuven, Belgium
[b] Université Libre de Bruxelles (ULB), Experimental Soft Matter and Thermal Physics group, Campus La Plaine, CP223, Boulevard du Triomphe, 1050 Brussels, Belgium.

*** Corresponding author**

Drs. Derick Yongabi
KU Leuven
Laboratory for Soft-Matter and Biophysics
Celestijnenlaan 200 D
B-3001 Leuven, Belgium
Tel: +3216376874
E-mail: derick.yongabi@kuleuven.be

Abstract: Understanding microbial adhesion and retention is crucial for controlling many processes, including biofilm formation, antimicrobial therapy as well as cell sorting and cell detection platforms. Cell detachment is inextricably linked to cell adhesion and retention and plays an important part in the mechanisms involved in these processes. Physico-chemical and biological forces play a crucial role in microbial adhesion interactions and altering the medium ionic strength offers a potential means for modulating these interactions. Real-time studies on the effect of ionic strength on microbial adhesion are often limited to short-term bacterial adhesion. Therefore, there is a need, not only for long-term bacterial adhesion studies, but also for similar studies focusing on eukaryotic microbes, such as yeast. Hereby, we monitored, in real-time, *S. cerevisiae* adhesion on gold and silica as examples of surfaces with different surface charge properties to disclose long-term adhesion, retention and detachment as a function of ionic strength using quartz crystal microbalance with dissipation monitoring. Our results show that short- and long-term cell adhesion levels in terms of mass-loading increase with increasing ionic strength, while cells dispersed in a medium of higher ionic strength experience longer retention and detachment times. The positive correlation between the cell zeta potential and ionic strength suggests that zeta potential plays a role on cell retention and detachment. These trends are similar for measurements on silica and gold, with shorter retention and detachment times for silica due to strong short-range repulsions originating from a high electron-donicity. Furthermore, the results are comparable with measurements in standard yeast culture medium, implying that the overall effect of ionic strength applies for cells in nutrient-rich and nutrient-deficient media.

Keywords: Cell adhesion, cell retention, cell detachment, QCM-D, biofilm formation, zeta potential, XDLVO theory

1. Introduction

Understanding microbial adhesion and detachment is crucial for many medical, industrial and environmental processes due to the involvement of these processes in biofilm formation [1]. In medical applications, such as intravascular catheters and prosthetic joints, biofilms often lead to infections that require expensive medical interventions [2]. Also, biofilms cause wound infections and are the leading cause of many human diseases, including bacterial endocarditis, and cystic fibrosis [3-5]. In addition, biofilms significantly affect the efficacy of antibiotics by sheltering bacteria from pharmaceuticals. Similarly, shielding of the host defence by the extracellular polymeric substances (EPSs) produced by cells during biofilm formation hinders the body's natural defence against disease [6]. Therefore, strategies that disrupt microbial ability to adhere to the host tissue are attractive for preventing infectious diseases and optimizing antimicrobial therapies [7]. From an environmental viewpoint, biofilms are beneficial in bioremediation applications and play an important role in the balance of the aquatic ecosystems [8]. However, in industrial processes, biofilms foul filtration membranes in water treatment systems, and reduce the efficiency of heat exchangers, thus causing poor performance and exerting a negative economic impact [1].

Controlling biofilm formation requires a solid understanding of the mechanisms of cell adhesion and detachment. Therefore, comprehensive models are needed that can explain and predict the initial attachment and subsequent cellular interactions with surfaces. Cell adhesion is driven by a physicochemical and biological interplay between cells and surfaces [9]. Two main theories are generally used to estimate the influence of physico-chemical properties on cell adhesion, being i) the thermodynamic approach and ii) the Derjaguin, Landau, Verwey, and Overbeek (DLVO) theory. According to the thermodynamic approach, adhesion is controlled by the balance between the interfacial free energies of the interacting bodies and the surrounding medium [10-12]. The DLVO theory states that adhesion is driven by the net cell-

substrate interactions [10]. This net interaction results from the balance between two additive forces, Lifshitz-van der Waals (LW) forces, which are generally short-ranged, and long-range electrostatic (EL) forces. LW forces are attractive and originate from weak interactions between neutral and stable molecules [10, 13]. The long-range electrostatic interactions result from the overlap between the electrical double layer of the cell and the substrate and can either be attractive or repulsive, depending on the charge of the substrate [9]. However, most natural surfaces are negatively charged and, because cells are also negatively charged, the long-range electrostatic forces are repulsive as a rule of thumb [9, 13]. At smaller cell-surface separations, the LW forces become more dominant and cells adhere, while at larger separations, the electrostatic repulsive interactions prevail [14]. An extended version of the DLVO theory, the so called "XDLVO", was developed to account for the influence of Lewis acid-base (AB) interactions. These interactions result in hydrophobic and hydrophilic (hydration) forces, which must be considered as well [10 -15].

A convenient way to control the net interactions is by modulating the electrostatic forces, and this can be achieved by tuning the ionic strength of the medium [15-20]. Increasing the ionic strength decreases the thickness of the double layer and the double layer repulsive influence decreases as a consequence [15-17]. The electrostatic interaction increases with an increase in the magnitude of the cell-surface zeta potential [9]. Previous studies indeed show that long-range electrostatic repulsion dominates at low ionic strengths, while at high ionic strengths, the Lifshitz van der Waals forces dominate [17-29]. For instance, experiments indicate that increasing the ionic strength from 0 to 0.3 M compresses the double layer and increases bacterial adhesion [12, 10, 20]. While electrostatic forces play an important role in cell attachment, AB interactions are the most predominant interactions between cells and surfaces in aqueous environments and represent up to about 90 % of all non-covalent interactions [15,

22, 23]. These interactions may therefore have a strong influence on the long-term adhesion behaviour of cells to surfaces [9].

Previous studies have employed techniques such as centrifuge and shear-force assays [24] to study the adhesion of cell populations, while for single cell studies, techniques including magnetic bead twisting cytometry [25], atomic force microscopy [26, 27], and optical trapping have been used [28]. Thermophoretic trapping is another potentially useful technique for manipulating micro- and nano-sized objects [29]. These methods are invasive and do not monitor the natural evolution of adhesion events in real time. Techniques capable of real-time monitoring without external perturbations are desired, as time is a crucial parameter in cell adhesion. A real-time monitoring technique based on interfacial thermal transport, the heat transfer method (HTM) has been used to detect cell-material interactions for a variety of cells [30-32]. The measurement technique involves a thermal gradient across the solid-liquid interface, meaning that the thermal gradient itself may be a source of hydro-thermodynamic perturbations, such as thermophoretic forces [29]. The quartz crystal microbalance with dissipation monitoring (QCM-D) circumvents these drawbacks, and, we therefore used it to probe the role of ionic strength on yeast adhesion over short (minutes to hours) and long (hours to days) time scales

While QCM-D studies have contributed to developing new microbial adhesion models [12, 33], further knowledge is still required on many aspects of microbial adhesion. For instance, with regards to the ionic strength, existing studies focus on bacteria, using techniques based on end point detection [18, 19] or focusing on initial bacterial attachment [12, 34-36]. Studies towards understanding the mechanisms of eukaryotic microbial adhesion as a function of ionic concentration over long time scales do not exist. Eukaryotic microbes, such as fungi also form biofilms and exist in environments with a wide range of salinities [37, 38]. For instance, biofilms formed by *Candida albicans* are the major cause of hospital-acquired infections [37].

Long-term surface-dependent adhesion and detachment of *S. cerevisiae* in PBS buffer was reported by Yongabi *et al*. in a comparative study including human embryonic kidney cells (HEK) and *E. coli* bacteria [39]. Ionic strengths vary markedly in many real-life situations [37-42]. Therefore, it is interesting to explore how these important adhesion events are modulated by ionic strength, both on the short- and long-term. For instance, in the human body, nutritional factors and disease conditions cause variation in the electrolyte concentration of extracellular fluid (ECF), which may in turn affect disease infections and therapies, with Na^+ and its counter anions being the most abundant ions [40, 41]. In addition, the bactericidal activity of human peripheral white blood cells (WBCs) has been linked to the concentration of Na^+ [40]. In the environment, the ionic strength in soil varies widely depending on varying degrees of snow-melting and rainfall (among other factors) which affects the adhesion of microorganisms. Furthermore, the salinity of freshwater and sea water differ markedly, which means that adhesion patterns of microorganisms are expected to be different between these environments.

In this study, we used *S. cerevisiae* as a model for eukaryotic microbial cells to monitor cell adhesion as a function of ionic strength. We chose *S. cerevisiae* because it is considered as the best model for studying eukaryotic cells due to its well-understood genetic sequence [43]. Similarly, the suitability of *S. cerevisiae* as a model for studying fungal biofilms is an added benefit [37, 44]. In addition, because of their well-known gene expression profiles, and the conservation of signalling pathways among yeast species, it is believed that studying *S. cerevisiae* might enable the identification of new therapeutic antifungal targets through the screening of molecules involved in the adhesion of fungi [37]. *S. cerevisiae* cells have a rigid cell wall (100 – 200 nm thick), which gives them their unique elliptical to ovoid shape and enables the cells to control their internal osmotic pressure by exhibiting a highly selective permeability to solutes through well-known mechanisms [9, 44-48]. This makes *S. cerevisiae* ideal for probing cell adhesion in a wide range of ionic strengths.

2 Materials and Methods

2.1 QCM-D measurements

QCM measurements were performed using a Q-sense E4 instrument acquired from Biolin Scientific (Gothenburg, Sweden). AT-cut quartz crystals (5 MHz resonance frequency, 14 mm diameter, 0.3 mm thickness purchased from the same company, with gold- and silica-coating (50 nm thickness), were used for adhesion monitoring. Gold and silica surfaces were used as they differ markedly in surface properties, such as surface charge, and surface hydrophobicity, which allows one to decouple the effect of these surface properties on the adhesion response [39]. Moreover, these materials are relevant for many biomedical applications, for example, in medical implants, and potentially for therapeutic purposes when in colloidal forms [49-54]. The Au- and SiO_2-coated crystals were cleaned as recommended by the manufacturer.

Adhesion measurements were performed by first stabilizing the frequency shift and energy dissipation in PBS for at least 20 min. After establishing a stable baseline in buffer, cell suspensions were added at a rate of 100 µL/min for 1 h to the sensor surface in a flow cell chamber (volume 40 µL). In order to eliminate any possible influence of the ionic strength on the QCM-D response, the initial stabilization step was carried out in PBS buffer of the same ionic strength as the medium in which the cells were suspended. After the cell addition step, the time-evolution of the frequency (Δf) and energy dissipation (ΔD) were monitored at the fundamental mode and several overtones (1^{st}, 3^{rd}, 5^{th}, 7^{th}, 9^{th}, 11^{th} and 13^{th}) to follow the different stages of cell adhesion in real time for at least 48 h without flow. Monitoring in the absence of flow means that we can exclude hydrodynamic effects on the measured adhesion events. Additional measurements were also performed in yeast peptone dextrose (YPD) medium to evaluate the effect of ionic strength on cell adhesion in a typical culture medium for yeast. All measurements were performed at 37 °C.

2.2. S. cerevisiae and cell preparation

We used baker's yeast *S. cerevisiae* from Dr. Oetker (Bielefeld, Germany). The cells are originally provided as small dry aggregates of rod-like shape. The physico-chemical properties of the yeast cells have been characterized in previous studies [39, 55, 56]. The yeast cells were rehydrated by dispersion in 1 × PBS at room temperature with gentle agitation for less than 1 min (vortexing, 500 rpm). Cells were then washed and harvested by centrifuging twice for 5 min each at 5000 rpm in 1 × PBS before resuspending in PBS with the desired ionic concentration. PBS solutions of different ionic concentrations were prepared by serial dilutions of 10 × PBS. 10 × PBS was prepared by dissolving a mixture of 37.7 g NaCl (> 99 % purity), 4.4 g Na_2HPO_4 (> 99 %), and 1 g KH_2PO_4 (> 99 % purity), all from Sigma-Aldrich (Overijse, Belgium) in 500 ml of deionized water (Milli-Q water). The pH of the 10 × PBS solution was adjusted to 7.4 to mimic the physiological value by adding NaOH and autoclaved for sterilization. The calculated ionic strengths are shown in **Table 1**. The dissociation state of the orthophosphoric acid is calculated via the Henderson-Hasselbalch equation, considering the effect of temperature and ionic strength (iteratively; I = 5) on the pKa values. Yeast adhesion and detachment was assessed for 6 ionic strengths ranging from 0 mM to 748 mM. An Ocean Optics™ Red Tide USB650 VIS-NIR Spectrometer was used to determine the concentrations of yeast cells. A concentration of 1.6×10^{5} cells/ml was used for all adhesion monitoring experiments.

Yeast extract, peptone and glucose were purchased from Sigma-Aldrich (Overijse, Belgium) and used to prepare Yeast Peptone Dextrose (YPD) culture medium according to the supplier's specifications in Milli-Q water and in media of different ionic strengths. All culture media were sterilized by autoclaving.

Table 1. *PBS buffer dilutions and corresponding ionic strengths*

PBS concentration (× PBS)	0	1	2	3	4	5	10
Ionic strength (mM)	0	149	299	449	598	748	1491

2.3. Zeta potential measurements

Zeta potentials were measured using a ZetaPlus zeta potential analyser (Brookhaven Instrument Corporation, NY, USA). Measurements were performed on cell suspensions consisting of ≈ 10^5 cells/mL at various ionic strengths. All measurements were carried out at 37 °C. For each measurement, the average zeta potential values were calculated from five runs.

2.4 Yeast cell viability analysis

Resazurin cell viability reagent (purity > 99%), purchased from Acros Organics (Thermo Fisher Scientific, Geel, Belgium) was used to assess the effect of ionic strength on yeast cell viability. Viable cells reduce the blue resazurin dye to pink resorufin, thus the amount of resorufin as a function of time is an indication of cell metabolic activity. A 15 µM resazurin solution was first prepared in PBS solutions of different ionic strengths (0 – 149 mM). To ensure that samples were sterilized, PBS was autoclaved while resazurin was filtered prior to use. Cell suspensions prepared in similar PBS buffers as the resazurin solution were incubated with the resazurin dye in a six-well plate and maintained at 37 °C for 3 hours. Afterwards, the fluorescence and absorbance of resorufin were measured from 100 µL aliquots every 20 min with a Tecan infinite 200PRO microwell plate reader (Tecan Trading AG, Männedorf, Switzerland) at 590 nm and 570 nm, respectively. Measurements were also performed for cells suspended in solutions with an ionic strength of 149 mM (1 × PBS), which displayed slightly different pH, ranging from pH 7 to 8 to exclude the effect of pH variation on the results of the viability test. To study the combined effect of elevated ionic strengths and the very long measurement time on cell

viability, we performed additional viability tests on cells extracted from the QCM-D device after adhesion monitoring for up to 4 days in 449 mM and 748 mM ionic strength buffers. Viability tests were performed on cells in suspension and on those that remained sticking on the QCM chip.

2.5 Atomic force microscopy

Atomic force microscopy (AFM) was used for surface roughness analyses of the gold and silica chips. Measurements were carried out in intermittent contact mode using an Agilent 5500 atomic force microscope (AFM) with MSNL-F cantilevers (f = 110 − 120 kHz, spring constant, k = 0.6 N/m, average tip radius = 2 − 12 nm). Gwyddion software was used to evaluate the AFM topography images [57].

2.6 Contact angle and acid-base surface tension (ST) measurements

Contact angle measurements were performed on clean Au and SiO_2 to ascertain their cleanliness and ensure that the two materials used for all measurements indeed exhibited the expected differences in terms of surface wetting and surface charge. The surfaces were cleaned as described in **Section 2.1**. Measurements were performed using the DataPhysics OCA 25 optical contact angle system (Filderstadt, Germany). Using the sessile drop method, a 5 µL-liquid drop (Milli-Q water) was dispensed at a rate of 1.00 µl/s. All measurements were performed in a temperature-stabilized room, with a room temperature of 18 °C.

In order to evaluate the effect of surface charge and consequently the role of hydration forces on the cell adhesion response from the substrate-surface perspective, we determined the surface tensions of the clean gold and silica surfaces according to the acid-base theory, which allows one to directly determine the electron-acceptor/electron-donor surface tensions. Therefore, in addition to measuring the water contact angles, two additional test liquids, namely diiodomethane (purity > 99 %) and

ethylene glycol (purity 99.8 %) both from Sigma-Aldrich (Overijse, Belgium) were used. The surface tension components of the test liquids are displayed in Table 2.

Table 2: *Test liquids and their surface tension (ST) components*

Liquid	ST total (mNm^{-1})	ST LW (mNm^{-1})	ST acid (mNm^{-1})	ST base (mNm^{-1})
Diiodomethane	50.8	50.8	0.7	0.0
Water	72.8	21.8	25.5	25.5
Ethylene glycol	48.0	29.0	3.0	30.1

2.7 Theoretical Background

According to the extended DLVO theory, the total interaction energy between a cell and a substrate, U^{Total} is the sum of the Lifshitz van der Waals interactions U^{LW}, electrostatic interactions U^{EL}, and the acid-base interactions U^{AB}. Based on the Derjaguin approximation, the interaction energies between a flat surface and spherical cells, with separation distance, h, can be estimated according to the following equations (See ref. 9 for more details).

$$U^{LW}(h) = 2\pi \Delta G_{l_0}^{LW} \frac{l_0^2 a_c}{h} \qquad \textbf{Eq. 1}$$

$$U^{AB} = 2\pi a_c \lambda \Delta G_{l_0}^{AB} e^{[(l_0 - h/\lambda)]} \qquad \textbf{Eq. 2}$$

Where λ is the decay length of the AB interactions, a_c the average radius of yeast cells, ΔG^{LW} and ΔG^{AB} the LW and AB free energies of adhesion per unit area, and l_0 the equilibrium distance [9, 13]. The electrostatic interactions can be determined through **Eq. 3**.

$$U^{EL}(h) = \pi \varepsilon_0 \varepsilon_r a_c \left[2 \Psi_s \Psi_c ln\left(\frac{1 + e^{-kh}}{1 - e^{-kh}}\right) + \left(\Psi_s^2 + \Psi_c^2\right) ln\left(1 - e^{-2kh}\right)\right] \qquad \textbf{Eq. 3}$$

Where k is the Debye screening parameter, while Ψ_c and Ψ_s are the surface potentials of the cell and substrate respectively. ε is the dielectric constant of the medium, and ε_0 the dielectric permittivity of vacuum. The surface potential is in turn related to the zeta potential according to **Eq. 4** [9], with Ψ and ζ being the surface and zeta potentials of the cell, respectively, and z the slipping distance. Therefore, the electrostatic interaction increases with an increase in the zeta potential. The Debye length (k^{-1}) is a good measure of the thickness of the double layer,

which in the case of a 1:1 electrolyte is given by **Eq. 5** [13]. Where c is the ionic concentration in mol l^{-1}, and N_A the Avogadro constant, ε the dielectric constant of the medium, ε_0 the dielectric permittivity of vacuum, k_B and T the Boltzmann constant and absolute temperature, respectively.

$$\Psi = \zeta\left(1 + \frac{z}{a_c}\right)e^{kz} \qquad \textbf{Eq. 4}$$

$$k = \sqrt{2000e^2 N_A c \Big/ \varepsilon\varepsilon_0 k_B T} \qquad \textbf{Eq. 5}$$

Therefore, the thickness of the double layer, k^{-1} is reciprocally proportional to the square root of the ionic concentration. This means that increasing the ionic concentration decreases the thickness of the double layer k^{-1}, and thus reduces the electrostatic double layer repulsive influence [15-17].

The ionic strength also moderates the AB interactions through changes in the electron accepting and donating properties of the cell and substrate surfaces [22, 23]. Thus, the role of ionic strength on each type of interaction must be taken into account, especially for measurements in aqueous media. This is important since AB interactions account for up to 90 % of all non-covalent interactions [22]. The interfacial tensions associated with the electron-acceptor and electron-donor properties of a surface can be directly determined using contact angle measurements and the acid-base approach [55, 58]. This method considers the total surface tension of a pure substance to be the sum of LW and AB components, with the AB components further split into electron-accepting (acid) and electron-donating (base) components. Therefore, with such measurements, the contribution of surface charge-related properties on the cell adhesion response can be assessed directly. A full treatment of the acid-base theory can be found in refs. [22, 23, 54, 55, 58].

3. Results and Discussion

3.1 Ionic strength and zeta potential of *S. cerevisiae*.

Fig. 1 shows the zeta potential of *S. cerevisiae* for various ionic strengths. Data points represent the averages of three measurements and the error bars are the standard deviations. As shown, the absolute value of the zeta potential decreases with increasing ionic strength from -18.6 ± 1.5 mV for Milli-Q water to nearly 0 mV for the highest ionic strengths. The solid line is a decaying exponential fit (R^2 = 0.96, reduced chi-square = 0.7). The effect of ionic strength on the zeta potential is stronger in the lower ionic strength regime because at low electrolyte concentrations, the charge on the cells is screened to a lesser extent. As charge screening increases due to high ionic concentration, the effect on the zeta potential gradually diminishes.

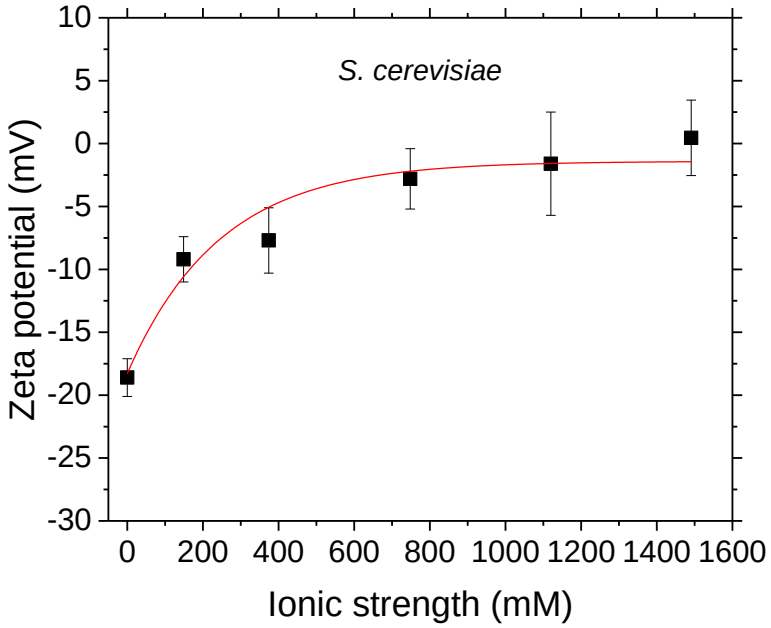

Fig. 1 *Ionic strength-dependent zeta potential of S. cerevisiae.*

The decrease in the zeta potential with increasing ionic strength is consistent with expectations from theory and previous measurements [9, 13]. The absolute values of the zeta potential also agree with measurements from literature. For instance, we recently measured a zeta potential of -9.0 ± 2 mV for yeast suspended in 149 mM ionic strength buffer [39]. Comparable zeta

potential values were also reported in ref. [55] (-9.4 ± 0.7 mV) and ref. [56] (-10 ± 1.3 mV) for yeast cells in 150 mM NaCl ionic strength media.

3.2 Ionic strength and *S. cerevisiae* viability

Table 2 shows yeast cell viability as a function of ionic strength. The resorufin fluorescence is highest in Milli-Q water (0 mM) and decreases with increasing ionic concentration, i.e., from 74 mM to 149 mM. Therefore, the viability of *S. cerevisiae* increases with decreasing ionic strength.

Table 3 *Dependence of cell viability on ionic strength.*

Dye incubation time (min)	**Sample**	**Fluorescence intensity (cps)**		
		0 mM	**74 mM**	**149 mM**
200	**PBS + dye**	**5109**	**5188**	**5080**
	Yeast suspension + dye	26040	6796	5449
220		29400	7417	5753
240		37950	9022	6407
260		44407	10190	6906

Table 3 also shows the fluorescence, in bold, measured with medium of the various ionic strengths incubated with resazurin without cells. The fluorescence intensity values are comparable, unlike the fluorescence values measured with cells in medium of the same ionic strengths. A fluorescence intensity of 18 cps was measured from an empty well. Therefore, the fluorescence differences measured from the cell suspensions are exclusively due to cellular activity. To ensure that small pH variations resulting from different dilutions did not affect the viability tests, we measured and analysed yeast cell viability in the 149 mM buffer while varying the pH within the range pH 7 – pH 8. Cell viability did not differ in this pH range.

3.3 Influence of ionic strength on yeast adhesion and detachment on gold

Fig. 2 shows a typical time-dependent frequency shift (**Fig. 2a**) and the associated energy dissipation (**Fig. 2b**) for a yeast adhesion measurement on gold over a period of 48 hours at 37 °C. Data from all overtones display similar patterns, and we focus on the middle overtone (7^{th}) for all analyses. The cells were dispersed in PBS of 149 mM ionic strength. The profile involves a stabilization period in pure PBS prior to a 1-hour cell addition period. The overall yeast cell adhesion profile under the same conditions of ionic strength and temperature has been previously described [39], where adhesion was divided into three stages, beginning with cell adsorption under flow, followed by steady-state adhesion during which cells spread and establish strong adhesion to the surface, and ending with cell detachment. As shown in **Fig. 2**, the maximum frequency shift for this measurement is 55.5 Hz, which is consistent with previous measurements using the same QCM-D device [39]. The cell retention time, defined as the time at which the magnitude of the frequency shift (Δf) attains its maximum value (Δf_{tot}) is 13.9 hours (see solid arrowhead in **Fig. 2a**). After this, cells detach to an extent quantified by the degree of Δf recovery [39]. The energy dissipation signal (ΔD) increases with decreasing Δf and attains a local maximum at the same time as Δf attains a maximum (in magnitude), which confirms that Δf changes are due to the adsorption and desorption of viscoelastic material, in this case, cells. Correlating the time dependence of Δf and ΔD can provide more information on cytoskeletal changes [39, 59, 60]. In this study, we focused on the frequency data only and all analysis are based on the 7^{th} overtone.

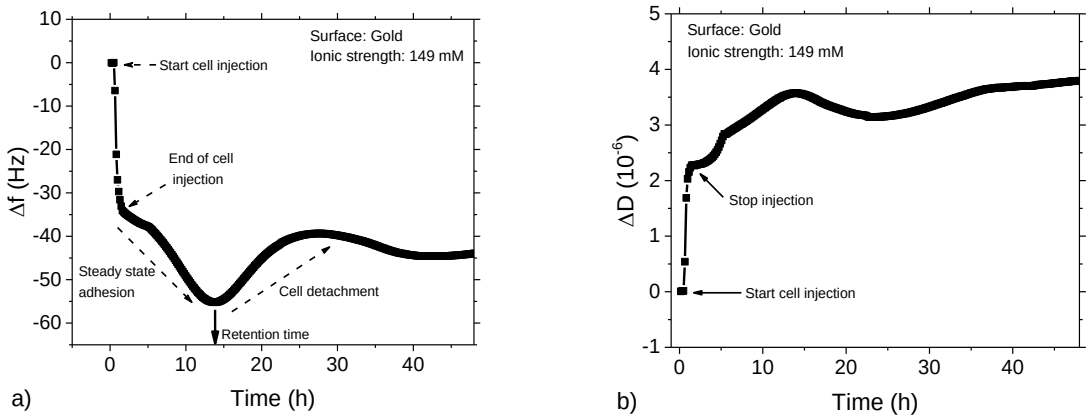

Fig. 2 *QCM-D monitoring of S. cerevisiae adhesion on gold. Frequency shift, Δf* ***(a)*** *and energy dissipation ΔD* ***(b)*** *for cells in 149 mM ionic strength buffer.*

Fig. 3a shows representative frequency shifts for long-term cell adhesion measurements performed for six different ionic strengths, including 0, 149, 299, 449, 598, and 748 mM. Interestingly, for each ionic strength, the adhesion and detachment phases described in **Fig. 2** can be identified. However, there are important differences when comparing the overall profiles by ionic strength. Henceforth, we focus on adhesion levels, retention and detachment times. The time-dependent frequency shift, Δf represents the adhesion level in terms of mass-loading, while the retention time corresponds to the maximum adhesion level (Δf_{tot}). The time taken for 50 % of the cells to detach, i.e, 50 % of Δf recovery will be referred to as the detachment time.

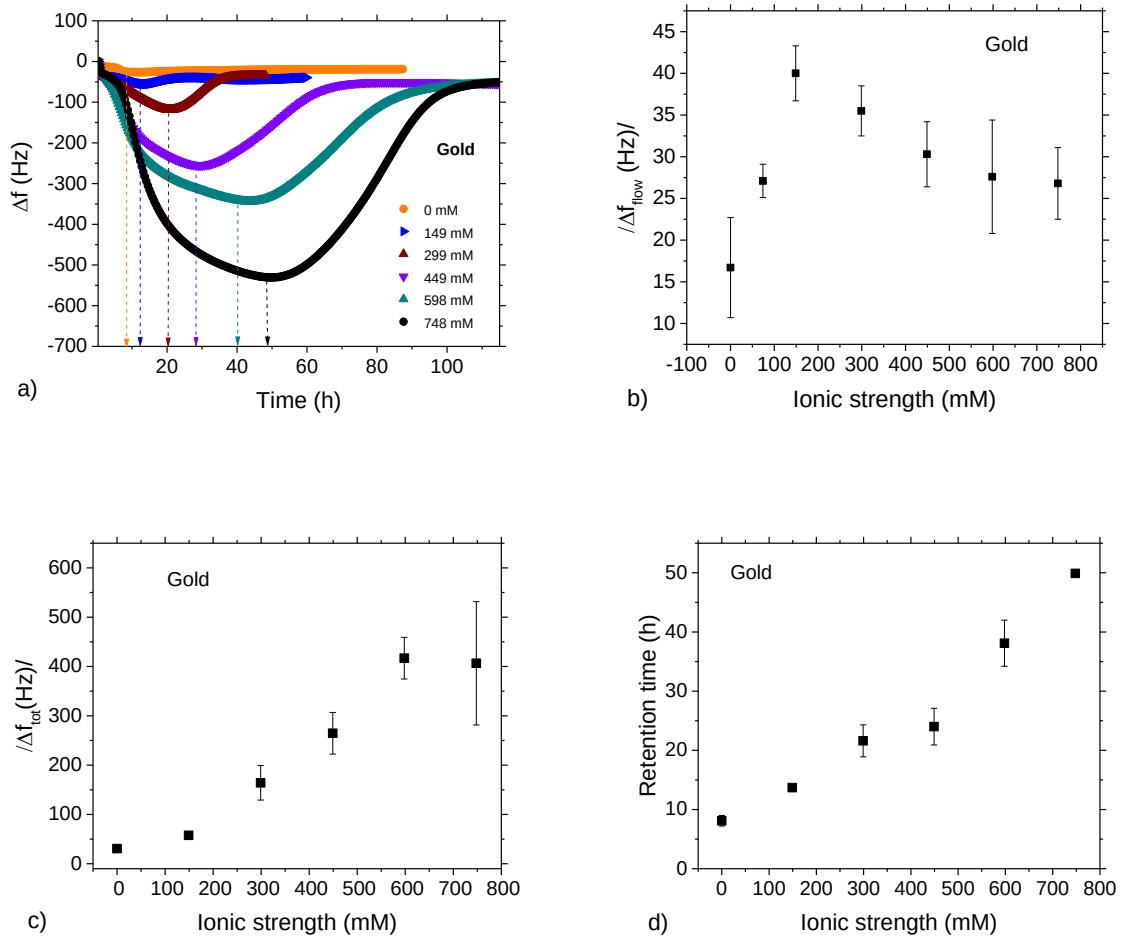

Fig. 3 *Ionic strength dependent yeast adhesion.* ***a)*** *Frequency shifts representing yeast adhesion levels and retention time as a function of ionic strength.* ***b)*** *Frequency shift resulting from 1-hour cell adsorption under flow.* ***c)*** *Maximum yeast adhesion (Δf_{tot}) as a function of ionic strength.* ***d)*** *Correlation between ionic strength and cell retention time. Error bars are the standard deviations from at least three measurements. For some data points, the error bars are smaller than the symbol size.*

3.3.1 Effect of ionic strength on *S. cerevisiae* adhesion and retention

The time-dependent frequency shifts represent the levels of cell adhesion as a function of time. The adhesion levels during the 1-hour cell injection period, Δf_{flow}, are markedly smaller for all ionic strengths compared to the total adhesion levels, Δf_{tot}. This confirms that the steady-state adhesion phase, which follows the end of cell injection, described in **Fig. 2a** and ref. [39] takes place for cells in all ionic strengths. **Fig. 3b** displays the average Δf_{flow} values from at least three

measurements, showing a clear increase in Δf from 0 mM to 149 mM, after which it decreases (additional data point for 74 mM included). The increasing trend is consistent with the sharp decrease in the magnitude of the zeta potential (**Fig. 1**), and thus indicates that this behaviour is largely due to a decrease in electrostatic repulsion as a result of charge screening. Calculations based on the DLVO theory show that for ionic strengths lower than 150 mM, the EL interactions are strong and decay more steeply as the ionic strength approaches 150 mM, thus explains the enhanced initial cell adhesion as the ionic strength increases in the 0 - 150 mM range [23]. This behaviour has also been reported in studies on bacteria, which show a general enhancement in adhesion as the ionic strength increases from 0 mM to 200 mM, due to a decrease in the thickness of the double layer to ≈ 0.7 nm [13, 23].

In terms of the yeast adhesion mechanisms, Castelain and co-workers employed optical trapping to show that different mechanisms are associated with different levels of ionic strengths between 0 and 150 mM. For instance, for an ionic strength of 1.5 mM, yeast cells were reported to undergo slipping and rolling while for 15 mM, they undergo not only slipping and rolling, but also sticking. For the much higher ionic strength of 150 mM, only sticking was observed [9]. The reason for the lower adhesion for ionic strengths above 150 mM is unclear and may reflect other adhesion mechanisms that come into play. Nevertheless, a similar decrease in the adhesion of *Vibrio alginolyticus* bacteria to hydroxyapatite has been reported for ionic strengths beyond 100 mM [13]. Furthermore, the adhesion behaviour reported in our study is in perfect agreement with results on dimyristoylphosphatidylserine (DMPS) vesicles adsorption on gold measured by Pramanik *et al.* [61]. The authors used DMPS vesicles as a model for Gram-negative bacteria and showed increased aggregation with increasing ionic strength up to 150 mM followed by a decrease for ionic strengths higher than 150 mM.

The total frequency shift, Δf_{tot} representing the overall adhesion in the long term shows a clear increase over the entire range of ionic strengths as displayed in **Fig. 3a**. **Fig. 3c** shows the average Δf_{tot} determined from three measurements as a function of ionic strength, with the error bars representing the standard deviations from at least three independent measurements. As displayed, Δf_{tot} increases with increasing ionic strength, with a behavior that is clearly different from the short-term trend. Based on these results, we can conclude that ionic strength promotes long-term cell adhesion levels within the concentration range used in this study. Because previous studies on the effect of ionic strength on eukaryotic cells have only focused on short term adhesion, references that correlate long-term cell adhesion and ionic strength are lacking. Our data however show that the enhancement of yeast adhesion due to an increase in ionic strength is not limited to initial cell attachment. Positive correlations between ionic strength and adhesion have also been reported for many bacteria species [62, 63].

The higher adhesion at elevated ionic strength seems to be unrelated to cell proliferation, since all measurements were performed in pure PBS and cells were washed before measurement as described in **Section 2.2**, hence no nutrients were available. In addition, the results from the cell viability analysis show that cell viability rather decreases with increasing ionic strength (see **Section 3.2**). A higher cell viability implies that cells have more energy to proliferate, thus the cell viability data, together with the absence of nutrients excludes the possibility that cell proliferation is involved in the higher signals measured at higher ionic strengths.

The arrowheads in **Fig. 3a** indicate the cell retention time for each ionic strength showing a clear change when varying ionic strength. **Fig. 3d** shows the cell retention time as a function of ionic strength from at least three measurements for each salinity level. As a general trend, the cell retention time increases markedly with increasing ionic strength. Therefore, unlike the trends in the initial adhesion (**Fig. 2b**), long-term adhesion shows a pronounced increase in both

cell adhesion levels and retention times throughout the wide range of ionic strengths studied. This confirms that other forces, beyond the classical DLVO forces must be important in driving yeast adhesion and retention on the long term. These are essentially acid-base interactions which are the dominant interaction forces between biological entities in aqueous media [22, 23]. These forces and their relevance to cell retention are explained in Section 3.3.2.

3.3.2 Ionic strength and *S. cerevisiae* detachment on gold

The detachment dynamics of *S. cerevisiae* cells was assessed by analysing the detachment phase of the time-dependent Δf profiles for all ionic strengths, except for Milli-Q water since the detachment is minimal in comparison with the overall adhesion. For this analysis, we applied a non-linear regression model to fit data covering the cell detachment phase using the Boltzmann function embedded in the OriginPro software package (OriginPro 2016®, version b9.3.226, Northampton, MA, USA). The fit function is given by **Eq. 6** and the fits are displayed by the solid lines in **Fig. 4a** ($R^2 \geq 0.999$ for all fits). The sigmoid nature of the profile indicates a cooperative process, in which the detachment of a few cells triggers the detachment of more cells [63, 64].

$$Y = A_2 + \frac{A_1 - A_2}{1 + \exp\left((t - t_{1/2})/\tau\right)} \qquad \text{Eq. 6}$$

Where A_1 and A_2 are the initial and final values of Y, in this case Δf, and $t_{1/2}$ is the absolute time at which the dependent variable Y is halfway between A_1 and A_2, τ is the time constant. $t_{1/2}$ and τ are unique parameters that can be used to evaluate the cell detachment dynamics as a function of ionic strength: $t_{1/2}$ is a good measure of the detachment time of the cell population, while τ characterises the detachment rate [39]. Here, we focus on the detachment half time, $t_{1/2}$ displayed in **Fig. 4b** for yeast adhesion on gold. Data points display the average of three measurements and the errors are the standard deviations. The results clearly show that the detachment time increases as the ionic strength increases.

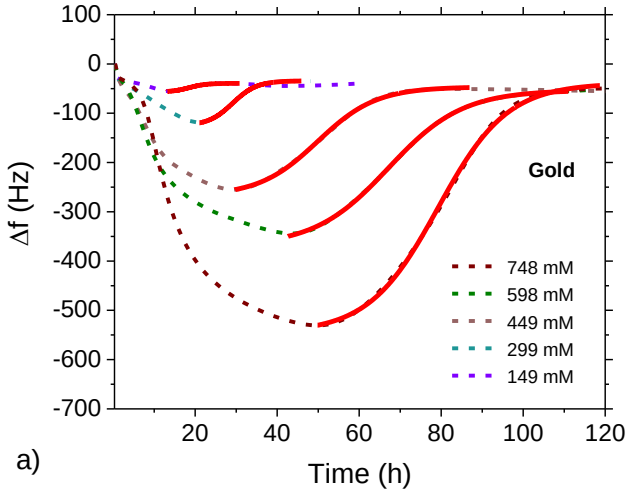

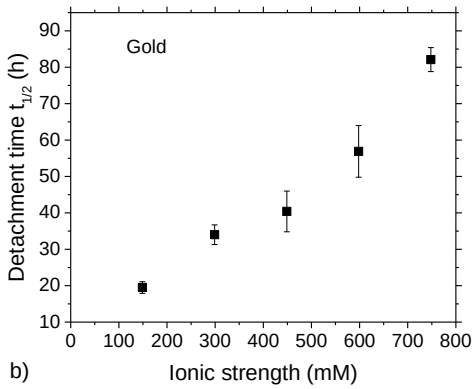

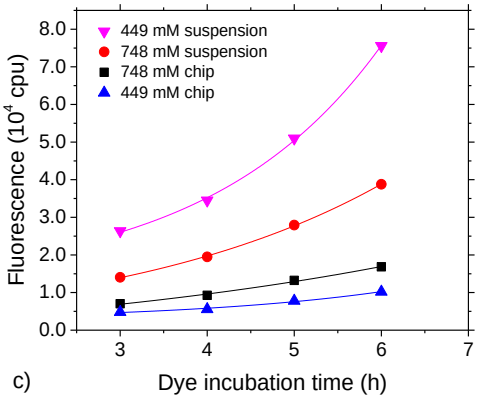

Fig. 4 *Ionic strength-dependent yeast detachment.* ***a)*** *Boltzmann fits of the detachment regime for various ionic strengths.* ***b)*** *Correlation between ionic strength and detachment time, showing an increase in detachment time with increasing ionic strength.* ***c)*** *Viability analysis of yeast cells after 4 days QCM-D measurements showing increasing viability as a function of the dye incubation time and proving that yeast cells remain viable over long measurement times in elevated ionic strength buffers. The fitted solid lines in c) are only for the purpose of guiding the eye.*

In general, the mechanisms behind cell detachment are not fully understood. However, cell detachment is an essential stage in biofilm formation and *S. cerevisiae* is known to form biofilms [15, 37]. Therefore, cells themselves may play an essential part in activating detachment, with the physico-chemical properties of the cell-medium and substrate-medium interfaces playing a strong moderating role. Based on the extended DLVO theory, these physico-chemical forces are essentially the Lewis acid-base, or electron–acceptor/electron–

donor interactions, which play a major role in determining cell fate on surfaces following initial cell attachment [9, 22]. This means that, while long-range electrostatic forces are relevant in cell adhesion, especially in initial cell attachment, they constitute only a small fraction of the total interactions, typically less than 10 times the Lewis acid-base forces within the 1-5 nm separations [23]. With regards to the influence of ionic strength, an increase in the ionic strength of the medium has been associated with alterations in the surface-charge properties and consequently AB interactions [66]. AB hydrophilic repulsions, which occur between hydrophilic bodies immersed in aqueous media are the main short-range forces counteracting the sustained adhesion of cells to surfaces [9, 23]. Hydrophilic repulsions arise when the electron accepticity of the surface is smaller than that of water and its electron donicity is higher than that of water [23]. In such cases, the surfaces attract water molecules more strongly than the cohesive AB attraction between the water molecules themselves. Highly hydrophilic surfaces with highly negative zeta potentials have a high electron donicity and therefore are more prone to hydrophilic repulsions [66]. The role of medium-ionic strength in moderating these short-range repulsive interactions was clearly demonstrated in Wu et al. They showed that the dominant effect of multivalent counterions in the presence of colloidal particles is the neutralization of AB sites on the particle surfaces, not the neutralization of the electrostatic charge. Specifically, they reported that in water, montmorillonite, glass and calcite particles exhibited strong AB repulsions, which transition into strong hydrophobic interactions upon addition of La^{3+} and Ca^{2+} ions. In addition, they showed that for the three particle types, the transition from hydrophilic repulsions to hydrophobic attractions correlated with the water contact angle of the surface, zeta potential of the surfaces as well as the value of the electron-donor component of the AB surface tension. For instance, for all three materials in water, they showed that the zeta potential and the electron- donor components of the AB surface tension are both high, which resulted in repulsive interactions, while in the presence of salt, both the

zeta potential and the electron-donor ST component decreased and resulted in particle adhesion. As explained in ref. [23], AB interactions also apply to biological entities, including cells. Yeast cell surfaces are hydrophilic with a contact angle in the range 25°- 42° [31, 39, 55] and as displayed in **Fig. 1**, the zeta potential of yeast in Milli-Q water is high, ≈ -19 mV and decreases with increasing ionic strength to ≈ - 2.5 mV for 748 mM. Therefore, in Milli-Q water, the cells are expected to experience strong hydrophilic repulsions, which are screened incrementally in the presence of salt, thus consistent with our results of longer retention/detachment times with increasing ionic strengths.

Biological process such as synthesis of adhesins and other yeast cell wall proteins are equally expected to play a major role in anchoring yeast cells to each other and to the surface [9, 67-69]. These cell-wall proteins are also important for cell spreading and cell-cell adhesion (flocculation) processes, which increase the anchorage and stability of the cell layer on the substrate. Such active biological processes, amongst others, evolve in time and space [69]. Furthermore, the cells themselves might play a role in their subsequent detachment by means of time-dependent disintegration of adhesion bonds or by the production of specific cell-wall entities, such as proteins, that alter the cell-substrate interfacial properties.

By performing additional cell viability measurements, we show that cells were still viable after being subjected to higher ionic strengths and long-term measurements. The results are displayed in **Fig. 4c** for cells adsorbed on a gold surface and in suspension after a 4-day measurement. Cells show continuous viability with time, for up to 6 hours following incubation in the dye. Overall, the viability is higher for cells measured in PBS of 449 mM ionic strength compared to cells in 748 mM ionic strength PBS, thus, consistent with the trends described in **Section 3.2**. The higher fluorescence from the cells on the gold chip can be attributed to a higher number of cells that remain sticking on the surface.

3.4 Correlation analysis

To compare the association between the ionic strength and total cell adhesion level, retention time and detachment time, we performed correlation tests. The correlation matrix is displayed in **Table 4**, which compares the correlation coefficients for the different pairs of variables. The data for all the parameters are normally distributed as determined from Shapiro-Wilk normality tests (p-value ≥ 0.1 for all tests). All correlation tests are statistically significant with p-values < 0.001. The ionic strength shows a strong positive correlation with adhesion levels, retention times and detachment times, with correlation coefficients of 0.97, 0.98 and 0.97 respectively. This analysis confirms that the trends in the overall adhesion levels, retention times and detachment times (all increasing with ionic strength) are indeed influenced by the ionic strength. In addition, the retention time and detachment times display a strong correlation (r = 0.99), with each also positively correlated with the total adhesion level, r = 0.95 for retention time and r = 0.93 for detachment time (**Table 4**).

Table 4*: Correlation (r values) of ionic strength with cell adhesion levels, retention and detachment times.*

	PBS dilution	**Ionic strength (mM)**	**Maximum adhesion (Δf_{tot}/Hz)**	**Retention time (h)**	**Detachment time (h)**
PBS dilution	1.000	1.000	0.974	0.976	0.967
Ionic Strength	1.000	1.000	0.974	0.976	0.967
Maximum adhesion	0.974	0.974	1.000	0.947	0.929
Retention time	0.976	0.976	0.947	1.000	0.993
Detachment time	0.967	0.967	0.929	0.992	1.000

3.5 Ionic strength and surface-dependent cell retention and detachment.

Surface properties, such as surface charge, zeta potential, hydrophilicity and surface roughness play important roles in the interaction of cells with surfaces. Therefore, we assessed the interplay between ionic strength and surface charge properties on cell retention and detachment by comparing yeast adhesion on silica and gold. Silica is very hydrophilic and highly polar compared to gold. For instance, as reported in ref. [39], silica is 4 time more polar than gold, with a polar surface free energy of 38 ± 3 mNm^{-1} (28.6 ± 1.5 mNm^{-1} dispersive), in comparison with 9.0 ± 1 mN m^{-1} for gold (40.4 ± 1.1 mNm^{-1} dispersive). To provide further insight into the surface charge properties of the silica and gold substrates, together with the nature and quantity of charge-related interaction energies in an aqueous medium, we performed contact angle and surface tension (ST) measurements on clean silica and gold surfaces as described in **Section 2.6**. As displayed in **Table 5**, compared to gold, the silica surface is very hydrophilic due to an electron-rich surface, evident from its high electron-donor (or base) ST. A very low electron-acceptor (or acid) ST is measured on both surfaces, indicating that the electron-donor components are the dominant AB interactions. Importantly, gold displays a larger LW ST component, which is consistent with the high dispersive surface free energy component measured on gold in previous studies [39].

Table 5: *Contact angle and surface tension (ST) components (LW, acid, and base) for gold and silica surfaces. Errors represent the standard deviations from three measurements.*

Surface	**Contact angle (°)**			**Surface tension (mNm^{-1})**			
	water	Ethylene glycol	Diiodomethane	Total	LW	Acid	Base
Silica	8 ± 1	5.7 ± 3	52.7 ± 7	48.4 ± 5	22.1 ± 4	2 ± 1	74.1 ± 0.4
Gold	63 ± 2	50.8 ± 5	23.1 ± 4	37 ± 4	37 ± 4	0.0	23.3 ± 1

The surface roughness of these materials can also significantly influence cell adhesion, thus, in addition, we assessed and compared their surface roughness. **Fig. 5** shows AFM images of the gold **(a)** and silica **(b)** QCM-chip surfaces displaying comparable surface roughness. For

instance, for the 1 µm profile shown in **Fig. 5c,** the root mean square (RMS) average values are 1.3 nm for gold and 1.4 nm for silica. Therefore, we expect minimal differences in relation to the effect of surface roughness on cell retention and detachment compared between gold and silica.

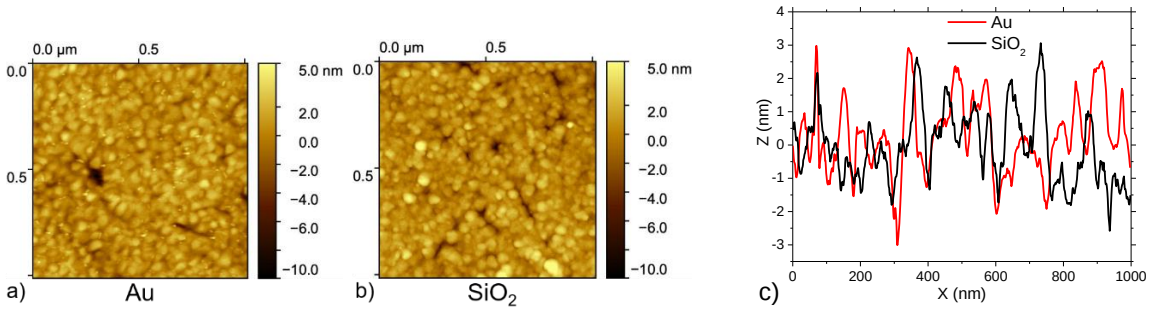

Fig. 5 *AFM analysis of Au* ***(a)*** *and* SiO_2 ***(b)*** *surfaces displaying comparable surface roughness as illustrated in the comparable line profiles in* ***c)****.*

Fig. 6a shows Δf vs time responses measured on silica for yeast dispersed in PBS of two ionic strengths, 149 mM and 299 mM over a period of 72 hours. Δf shows larger changes and a longer retention time for 299 mM compared to 149 mM. **Fig. 6b** compares Δf vs time plots between gold and silica for the two ionic strengths: For each ionic strength, the maximum frequency shift is higher for silica than for gold. The results for 149 mM agree with the findings from ref. [39], in which a higher adhesion of eukaryotic cells (*S. cerevisiae* yeast and human embryonic kidney cells) on silica was reported in comparison with gold.

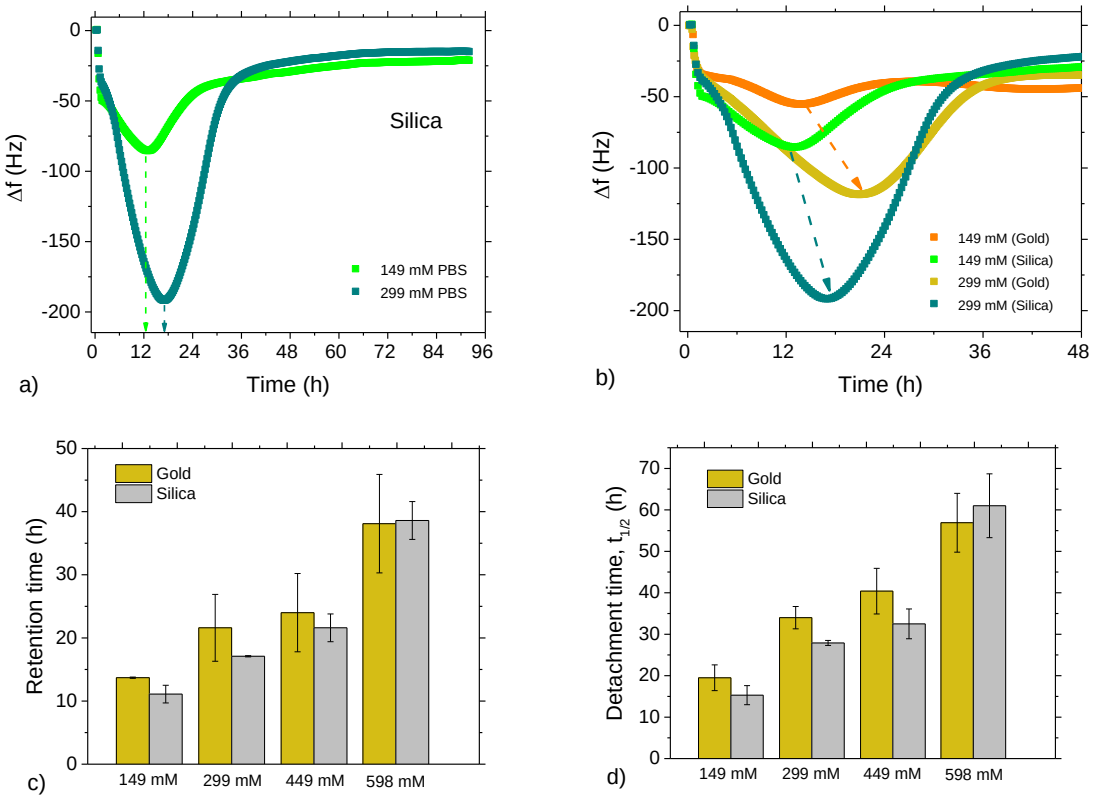

Fig. 6 *Comparison of ionic strength-dependent yeast retention and detachment on gold and silica surfaces.* ***a)*** *Yeast adhesion levels and retention time on silica both increase with ionic strength.* ***b)*** *Comparison of Δf between silica and gold, depicting shorter retention times on silica for 149 mM PBS and 299 mM PBS.* ***c)*** *Ionic strength-dependent retention times on silica and gold displaying similar trends with shorter times for silica.* ***d)*** *Comparison of cell detachment time between gold and silica showing an increase for both surfaces with ionic strength. Error bars are standard deviations from at least three measurements.*

Fig. 6b also displays an increase in the retention times (arrowed lines), which are longer for 299 mM PBS compared to 149 mM for both gold and silica. The retention time in each case is longer for gold than for silica. **Fig. 6c** compares the ionic strength dependence of cell retention time between the two surfaces for ionic strengths up to 598 mM. First, it is clear that for silica, the retention time increases with ionic strength in a similar manner as described for gold in **Section 3.3.1** (**Fig. 3c**). Comparing gold and silica, as a general trend, the retention time measured on silica is shorter than the corresponding value on gold (**Fig. 6c)**. This difference

seems to diminish at higher ionic strength, e.g., for 598 mM ionic strength. **Fig. 6d** compares the detachment time $t_{1/2}$ between gold and silica as a function of ionic strength. The $t_{1/2}$ values for silica were determined in the same way as described for gold in **Section 3.3.2**. For silica, the detachment time trend over the entire range of ionic strengths closely resembles that observed for gold. This means that the influence of ionic strength on the cell detachment time is strong for both surfaces. The shorter retention times on silica can be attributed to stronger AB repulsive forces between the cells and the surface. As shown in **Table 5**, the electron-donor component of the AB interactions, which is responsible for the hydrophilic repulsions is over 3 times larger on silica (74.1 ± 0.4 mNm^{-1}) compared to gold (23.3 ± 1 mNm^{-1}). The fact that at higher ionic strengths, the difference in cell retention and detachment times diminishes when compared between gold and silica suggests that at such ionic strength, electron-donor sites on the silica surface are fully compensated. Additionally, the positive correlation between surface zeta potential and hydration force as a function of ionic strength as demonstrated in ref. [66] indicates that measuring the zeta potential of the surfaces as a function of ionic strength under similar QCM-D measuring conditions may provide further insights into the fundamental mechanisms responsible for the surface-dependence of cell retention and detachment. Importantly, for gold, the high LW ST component, which is associated with LW attractive forces provides an additional explanation for the longer retention times/delayed detachment of *S. cerevisiae* on gold.

Cell viability is also an important parameter in the overall cell adhesion response. Therefore, the effect of substrate surface chemistry on cell viability should be considered as well. For instance, studies on mammalian cells (Cell line L929) reported a decrease in cell viability on super hydrophilic surfaces based on titanium [70]. However, the correlation between contact angle and cell viability can vary between different materials. Moreover, the tolerance level of cells to extreme physico-chemical conditions is cell-type specific: *S. cerevisiae* cells for

instance are considerably more tolerant due to their rigid cell walls in comparison to mammalian cells. In this study, we observe similar adhesion and detachment trends on silica and gold as a function of ionic strength. Secondly, our measurements show that for high ionic strengths, cell viability is low (See **Table 3**, **Fig. 4c**), but cell retention and detachment times are significantly longer than with low salinity. Therefore, it is less likely that the shorter retention and detachment times measured on silica is a consequence of decreased cell viability. Overall, this indicates that it would certainly be worthwhile to study additional combinations of cell- and substrate-types to identify possible underlying patterns.

3.6 Influence of nutrients

All measurements described in **Sections 3.1** to **3.5** were performed in pure PBS to eliminate the effect of complex media on the cell-material interactions [61]. The presence of complex media can hinder the monitoring of cell adhesion behaviour when using techniques that depend on mass loading. This is because in the presence of medium, a significant contribution of the measured QCM-D response originates from the adsorbed layer of proteins and other materials. Therefore, it is interesting and relevant to assess whether the results apply in more complex media.

Fig. 7a shows the adsorption of culture medium onto a gold chip (black curve), which was first stabilized for 30 min in 149 mM ionic strength PBS before adding culture medium. As shown, the frequency decreases to -54 Hz following the addition of culture medium and remains constant throughout the entire 6-day measurement time.

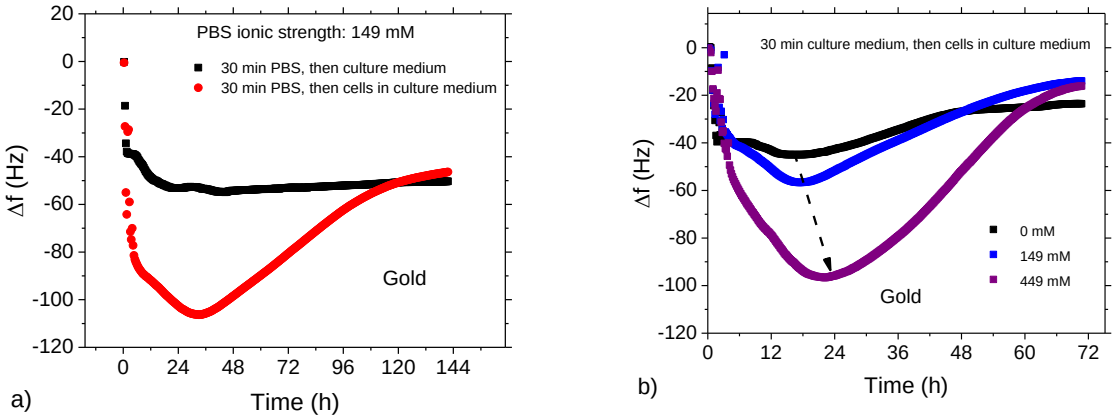

Fig. 7 *Effect of culture medium on yeast adhesion and detachment.* ***a)*** *Comparison of frequency shifts resulting from the exchange of pure PBS (149 mM) with culture medium of 149 mM ionic strength (black upper curve) and yeast cells in 149 mM-culture medium (red lower curve). Culture medium contributes to the overall cell-material interactions for cells in a culture-rich environment.* ***b)*** *Cell adhesion level and retention time also increase with increasing ionic strength for cells suspended in culture medium.*

The red curve displays the frequency response measured with cells. Similarly, the QCM-D response was first stabilized in pure PBS of 149 mM ionic strength in the measuring cell compartment before adding cells in 149 mM ionic strength-culture medium. The frequency shift is twice the value measured with the culture medium-only sample. Since both measurements involved an initial stabilization in 149 mM ionic strength PBS, the contribution due to cells is the difference, which is ≈ - 54 Hz and comparable with the value of -55 Hz measured for cells suspended in pure PBS on gold as described in **Section 3.3**. This shows clearly that measurements involving complex media give results that have contributions from both cells and medium interactions. Importantly, the frequency response with cells displays the typical adhesion and detachment profiles described for cells in pure PBS. The absence of a detachment phase for the culture medium sample (without cells) confirms that the recovery phase measured with cells is exclusively due to cell detachment [39]. Similar to measurements in pure PBS, ionic strength also controls the cell adhesion levels and detachment times as shown in **Fig. 7b**. All measurements in **Fig. 7b** were performed by first stabilizing the QCM-D

response in culture media of the respective ionic strengths for 30 mins before injecting cells suspended in culture media prepared in buffers of the corresponding ionic strengths. For each ionic strength, the frequency response displays profiles similar to those obtained for cells dispersed in pure PBS. As displayed, adhesion levels and the cell retention time both increase with ionic strength. Therefore, cell adhesion, as well as long term retention and detachment are controlled by ionic strength in both nutrient-free and nutrient-rich media. Pure cell material interactions in PBS yield significantly shorter retention times. This time becomes markedly prolonged in the presence of nutrients, an effect that can be attributed to either additional interactions from medium macromolecules, i.e., macromolecular-cell and macromolecular-substrate interactions or biological processes, such as enhanced expression of surface molecules (e.g, proteins).

Conclusion

The effect of ionic strength on microbial-surface interactions is customarily restricted to bacterial adhesion at short time scales, while the long-term effects have been traditionally not taken into account. In this work we have extended the study of real-time cellular adhesion and detachment to long term for eukaryotic microbes. Specifically, we have explored the effect of ionic strength on *S. cerevisiae* adhesion, retention and detachment as an example of a eukaryotic microbial cell.

Our QCM-D results reflect the strong influence of ionic strength on cell adhesion over long-time scales, namely, adhesion levels increase strongly with ionic strength. Cell retention and detachment times also display a positive correlation with ionic strength. The presence of salt strongly modulates the acid-base interactions at the cell-liquid interface through a reduction of the electron-donor component of the interfacial energy. As a consequence, the short-range hydrophilic repulsions diminish incrementally with increasing ionic strength. Because the interaction energy is a balance between the hydrophilic repulsions and hydrophobic forces, the

net interactions become more and more hydrophobic with increasing salt concentration, thus resulting in enhanced cell-substrate retention, and delayed detachment.

Measurements performed on gold and silica, used as examples of surfaces differing in surface charge display (qualitatively) similar positive trends of cell adhesion as well as cell retention and detachment with ionic strength. However, in terms of absolute retention and detachment times, the values are shorter for measurements on silica in comparison with gold, which can be attributed to the fact that the silica surface has a much higher electron-donor surface tension component that is directly associated with a strong short-range hydrophilic repulsive force. This component is much smaller for gold, and on top of that, gold has a large LW attractive contribution to its total surface tension interactions. However, these differences become less clear for much elevated ionic strengths, probably due to a full compensation of electron donor sites on silica. Furthermore, we demonstrate that our results can be generalized from culture-free to culture-rich media in terms of the overall long-term adhesion and detachment profile, and in relation to the positive correlation between ionic strength and the different adhesion events, namely, the adhesion levels, retention times and detachment times.

Cell adhesion and detachment processes are important steps in the formation of biofilms, and thus, these results might not only shed more light on biofilm formation mechanisms and disease pathogenesis in environments within a wide range of salinity gradients, but also highlight potential new strategies for disrupting the ability of microbes to adhere and form biofilms on biological, as well as biomedical and industrial materials. Finally, the ability to modulate cell adhesion by tuning the ionic strength provides a potential strategy for developing optimized cell sorting and cell detection platforms. This is particularly useful for detecting trace-level cells, since higher ionic strengths may boost the detection limits due to an increase in adhesion interactions.

Acknowledgements

This work was financed by the KU Leuven project C14/15/066 “Smart Cellular Scaffolds” and the Research Foundation Flanders FWO, project G.0791.16N “Utilizing interfacial impedance- and heat-transfer phenomena in advanced monitoring- and switching devices”. Olivier Deschaume and Carmen Bartic acknowledge the funding by FWO Flanders (G0947.17N, 1SC3819N) and KU Leuven BOF grants C14/18/061 and C14/16/063. The authors would like to thank Prof. Dr. Liesbet Lagae and Tim Steylaerts (both in IMEC, Belgium) for providing access to the QCM-D instrument and Prof. Dr. Marlies Van Bael (Hasselt University) for providing access to the zeta potential analyser. We also thank Prof. Dr. Kevin Verstrepen (KU Leuven and Flemish Institute of Biotechnology VIB) and Drs. Alessia Gennaro (KU Leuven) for stimulating discussions.

References

1 J.W. McClaine, R.M. Ford. Reversal of flagellar rotation is important in initial attachment of *Escherichia coli* to glass in a dynamic system with high-and low-ionic-strength buffers. Appl. Environ. Microbiol. 68 (2002) 1280-1289.

2 J. Groll, J. Fiedler, K. Bruellhoff, M. Moeller, R.E. Brenner. Novel surface coatings modulating eukaryotic cell adhesion and preventing implant infection. Int. J. Artif. Organs 32 (2009) 655-662.

3 T.R. Garrett, M. Bhakoo, Z. Zhang. Bacterial adhesion and biofilms on surfaces. Prog. Nat. Sci. 18 (2008) 1049-1056.

4 J. Pizarro-Cerdá, P. Cossart. Bacterial adhesion and entry into host cells. Cell 124 (2006) 715-727.

5 M.R. Parsek, P.K. Singh. Bacterial biofilms: An emerging link to disease pathogenesis. Annu. Rev. Microbiol. 57 (2003) 677-701.

6 J.W. Costerton, P.S. Stewart, E.P. Greenberg. Bacterial biofilms: A common cause of persistent infections. Science 284 (1999) 1318-1322.

7 I. Ofek, I. Kahane, N. Sharon. Toward anti-adhesion therapy for microbial diseases. Trends Microbiol. 4 (1996) 297-299.

8 M.E. Witt, M.J. Dybas, D.C. Wiggert, C.S. Criddle. Use of bioaugmentation for continuous removal of carbon tetrachloride in model aquifer columns. Environ. Eng. Sci. 16 (1999) 475-485.

9 M. Castelain, F. Pignon, J.M. Piau, A. Magnin. The initial single yeast cell adhesion on glass via optical trapping and Derjaguin–Landau–Verwey–Overbeek predictions. J. Chem. Phys. 128 (2008) 135101.

10 A. Vilinska, K.H. Rao. Surface thermodynamics and extended DLVO theory of Leptospirillum ferrooxidans cells' adhesion on sulfide minerals. Mining Metall. Explor. 28 (2011) 151-158.

11 D.R. Absolom, F.V. Lamberti, Z. Policova, W. Zingg, C.J. van Oss, A.W. Neumann. Surface thermodynamics of bacterial adhesion. Appl. Environ. Microbiol. 46 (1983) 90-97.

12 K. Otto, H. Elwing, M. Hermansson. Effect of ionic strength on initial interactions of *Escherichia coli* with surfaces, studied on-line by a novel quartz crystal microbalance technique. J. Bacteriol. 181 (1999) 5210-5218.

13 M. Hermansson. The DLVO theory in microbial adhesion. Colloids Surf. B 14 (1999) 105-119.

14 K. Hori, S. Matsumoto. Bacterial adhesion: from mechanism to control. Biochem. Eng. J. 48 (2010) 424-434.

15 S. Achinas, N. Charalampogiannis, G.J.W. Euverink. A brief recap of microbial adhesion and biofilms. Appl. Sci. 9 (2019) 2801.

16 M. Fletcher, D.C. Savage. Bacterial Adhesion: Mechanisms and Physiological Significance. Springer Science & Business Media, Berlin, Germany, 2013.

17 J.N. Israelachvili. Intermolecular and surface forces, 2nd edn. Academic Press, San Diego, CA 1992.

18 H.H. Rijnaarts, W. Norde, J. Lyklema, A.J. Zehnder. DLVO and steric contributions to bacterial deposition in media of different ionic strengths. Colloids Surf. B 14 (1999) 179-195.

19 V. Vadillo-Rodriguez, H.J. Busscher, H.C. van der Mei, J. de Vries, W. Norde. Role of *Lactobacillus* cell surface hydrophobicity as probed by AFM in adhesion to surfaces at low and high ionic strength. Colloids Surf. B 41 (2005) 33-41.

20 M.J. Gross, B.E. Logan. Influence of different chemical treatments on transport of *Alcaligenes paradoxus* in porous media. Appl. Environ. Microbiol. 61 (1995) 1750-1756.

21 C.J. van Oss. Energetics of cell-cell and cell-biopolymer interactions. Cell Biophys. 14 (1989) 1-16.

22 D. Grasso, K. Subramaniam, M. Butkus, K. Strevett, J. Bergendahl. A review of non-DLVO interactions in environmental colloidal systems. Rev. Environ. Sci. Biotechnol. 1 (2002) 17-38.

23 C.J. van Oss. Long-range and short-range mechanisms of hydrophobic attraction and hydrophilic repulsion in specific and aspecific interactions. J. Mol. Recognit. 16 (2003) 177-190.

24 R. Ungai-Salánki, B. Peter, T. Gerecsei, N. Orgovan, R. Horvath, B. Szabó. A practical review on the measurement tools for cellular adhesion force. Adv. Colloid Interface Sci. 269 (2019) 309-333.

25 N. Wang, J.P. Butler, D.E. Ingber. Mechanotransduction across the cell surface and through the cytoskeleton. Science 260 (1993) 1124-1127.

26 P.H. Puech, A. Taubenberger, F. Ulrich, M. Krieg, D.J. Muller, C.P. Heisenberg. Measuring cell adhesion forces of primary gastrulating cells from zebrafish using atomic force microscopy. J. Cell Sci. 118 (2005) 4199-4206.

27 W.R. Bowen, R.W. Lovitt, C.J. Wright. Atomic force microscopy study of the adhesion of *Saccharomyces cerevisiae*. J. Colloid Interface Sci. 237 (2001) 54-61.

28 A.L. Birkbeck, R.A. Flynn, M. Ozkan, D. Song, M. Gross, S.C. Esener. VCSEL arrays as micromanipulators in chip-based biosystems. Biomed. Microdevices 5 (2003) 47-54.

29 M. Braun, F. Cichos. Optically controlled thermophoretic trapping of single nano-objects. ACS Nano 7 (2013) 11200-11208.

30 P. Cornelis, S. Givanoudi, D. Yongabi, H. Iken, S. Duwé, O. Deschaume, J. Robbens, P. Dedecker, C. Bartic, M. Wübbenhorst, M.J. Schöning, M. Heyndrickx, P. Wagner. Sensitive and specific detection of *E. coli* using biomimetic receptors in combination with a modified heat-transfer method. Biosens. Bioelectron. 136 (2019) 97-105.

31 D. Yongabi, M. Khorshid, Losada-Pérez P, Eersels K, Deschaume O, D'Haen J, Bartic C, Hooyberghs J, Thoelen R, Wübbenhorst M, Wagner P. Cell detection by surface imprinted polymers SIPs: A study to unravel the recognition mechanisms. Sens. Actuator B-Chem. 255 (2018) 907-917.

32 K. Eersels, B. van Grinsven, A. Ethirajan, S. Timmermans, K.L. Jiménez Monroy, J.F. Bogie, S. Punniyakoti, T. Vandenryt, J.J. Hendriks, T.J. Cleij, M.J. Daemen, V. Somers, V. De Ceuninck, P. Wagner. Selective identification of macrophages and cancer cells based on thermal transport through surface-imprinted polymer layers. ACS Appl. Mater. Interfaces 5 (2013) 7258-7267.

33 A. Tarnapolsky, V. Freger. Modeling QCM-D response to deposition and attachment of microparticles and living cells. Anal. Chem. 90 (2018) 13960-13968.

34 J. Gutman, S.L. Walker, V. Freger, M. Herzberg. Bacterial attachment and viscoelasticity: Physicochemical and motility effects analyzed using quartz crystal microbalance with dissipation (QCM-D). Environ. Sci. Technol. 47 (2013) 398-404.

35 A.L. Olsson, H.C. Van der Mei, H.J. Busscher, P.K. Sharma. Acoustic sensing of the bacterium–substratum interface using QCM-D and the influence of extracellular polymeric substances. J. Colloid Interface Sci. 357 (2011) 135-138.

36 J. Strauss, Y. Liu, T.A. Camesano. Bacterial adhesion to protein-coated surfaces: An AFM and QCM-D study. JOM. 61 (2009) 71-74.

37 G. Guillemot, G. Vaca-Medina, H. Martin-Yken, A. Vernhet, P. Schmitz, M. Mercier-Bonin. Shear-flow induced detachment of *Saccharomyces cerevisiae* from stainless steel: influence of yeast and solid surface properties. Colloids Surf. B 49 (2006) 126-135.

38 F.B. Kakahi, S. Ly, C. Tarayre, O. Deschaume, C. Bartic, P. Wagner, P. Compère, G. Derdelinckx, C. Blecker, F. Delvigne. Modulation of fungal biofilm physiology and secondary product formation based on physico-chemical surface properties. Bioproc. Biosyst. Eng. 42 (2019) 1935-1946.

39 D. Yongabi, M. Khorshid, A. Gennaro, S. Jooken, S. Duwé, O. Deschaume, P. Losada-Pérez, P. Dedecker, C. Bartic, M. Wübbenhorst, P. Wagner. QCM-D study of time-resolved cell adhesion and detachment: Effect of surface free energy on eukaryotes and prokaryotes. ACS Appl. Mater. Interfaces 12 (2020) 18258-18272.

40 L. Sobotka, S. Allison, Z. Stanga. Basics in clinical nutrition: Water and electrolytes in health and disease. Eur. E J. Clin. Nutr. Metab. 6 (2008) e259-e266.

41 R.W. Schrier. Diagnostic value of urinary sodium, chloride, urea, and flow. J. Am. Soc. Nephrol. 22 (2011) 1610-1613.

42 J.P. Mizgerd, L. Kobzik, A.E. Warner, J.D. Brain. Effects of sodium concentration on human neutrophil bactericidal functions. Am. J. Physiol. 269 (1995) L388-L393.

43 D. Botstein, G.R. Fink. Yeast: an experimental organism for 21st Century biology. Genetics 189 (2011) 695-704.

44 T.B. Reynolds, G.R. Fink. Bakers' yeast, a model for fungal biofilm formation. Science 291 (2001) 878-881.

45 F. Li, S.P. Palecek. EAP1, a *Candida albicans* gene involved in binding human epithelial cells. Eukaryot. Cell 2 (2003) 1266-1273.

46 G.M. Walker. Yeast Physiology and Biotechnology. John Wiley & Sons, Chichester, UK, 1998.

47 A.E. Smith, Z. Zhang, C.R. Thomas, K.E. Moxham, A.P. Middelberg. The mechanical properties of *Saccharomyces cerevisiae*. Proc. Natl. Acad. Sci. U S A 97 (2000) 9871-4.

48 A.J. Meikle, R.H. Reed, G.M. Gadd. Osmotic adjustment and the accumulation of organic solutes in whole cells and protoplasts of *Saccharomyces cerevisiae*. Microbiology 134 (1988) 3049-3060.

49 M. Saini, Y. Singh, P. Arora, V. Arora, K. Jain. Implant biomaterials: A comprehensive review. World J. Clin. Cases 3 (2015) 52-57.

50 H.J. Brandon, V.L. Young, K.L. Jerina, C.J. Wolf. Analysis of explanted silicone/silica composite breast implants. Adv. Compos. Lett. 9 (2000) 115-123.

51 J. Ballarre, S.M. Ceré. In L. Klein, M. Aparicio, A. Jitianu (editors), Handbook of Sol-Gel Science and Technology: Processing, Characterization and Applications. Springer, Cham, Switzerland, 2018. Chapter 121.

52 S.H. Jun, E.J. Lee, S.W. Yook, H.E. Kim, H.W. Kim, Y.H. Koh. A bioactive coating of a silica xerogel/chitosan hybrid on titanium by a room temperature sol–gel process. Acta Biomater. 6 (2010) 302-307.

53 M. Vallet-Regí, F. Balas. Silica materials for medical applications. Open Biomed. Eng. J. 2 (2008) 1-9.

54 H.H. Wang, C.H. Su, Y.J. Wu, C.A.J. Lin, C.H. Lee, J.L. Shen, W.H. Chan, W.H. Chang, H.I. Yeh. Application of gold in biomedicine: Past, present and future. Int. J. Gerontol. 6 (2012) 1-4.

55 S. Kang, H. Choi. Effect of surface hydrophobicity on the adhesion of *S. cerevisiae* onto modified surfaces by poly (styrene-ran-sulfonic acid) random copolymers. Colloids Surf. B 46 (2005) 70-77.

56 M. Castelain, P.G. Rouxhet, F. Pignon, A. Magnin, J.M. Piau. Single-cell adhesion probed in-situ using optical tweezers: A case study with *Saccharomyces cerevisiae*. J. Appl. Phys. 111 (2012) 114701.

57 D. Nečas, P. Klapetek. Gwyddion: An open-source software for SPM data analysis. Open Phys. 10 (2012) 181-188.

58 C.J. Van Oss, R.J. Good, M.K. Chaudhury. The role of van der Waals forces and hydrogen bonds in "hydrophobic interactions" between biopolymers and low energy surfaces. J. Colloid Interface Sci. 111(1986) 378-390.

59 S. Zhang, H. Bai, P. Yang. Real-time monitoring of mechanical changes during dynamic adhesion of erythrocytes to endothelial cells by QCM-D. Chem. Commun. 51 (2015) 11449-11451.

60 T. Zhou, K.A. Marx, A.H. Dewilde, D. McIntosh, S.J. Braunhut. Dynamic cell adhesion and viscoelastic signatures distinguish normal from malignant human mammary cells using quartz crystal microbalance. Anal. Biochem. 421 (2012) 164-171.

61 S.K. Pramanik, S. Seneca, A. Ethirajan, S. Neupane, F.U. Renner, P. Losada-Pérez. Ionic strength dependent vesicle adsorption and phase behavior of anionic phospholipids on a gold substrate. Biointerphases 11 (2016) 019006.

62 C.R. Bunt, D.S. Jones, I.G. Tucker. The effects of pH, ionic strength and polyvalent ions on the cell surface hydrophobicity of Escherichia coli evaluated by the BATH and HIC methods. Int. J. Pharm. 113(1995) 257-261.

63 B. Li, B.E. Logan. Bacterial adhesion to glass and metal-oxide surfaces. Colloids Surf. B 36(2004) 81-90.

64 A. Whitty. Cooperativity and biological complexity. Nat. Chem. Biol. 4 (2008) 435-439

65 K.A. Marx, T. Zhou, M. Warren, S.J. Braunhut. Quartz crystal microbalance study of endothelial cell number dependent differences in initial adhesion and steady-state behavior: evidence for cell-cell cooperativity in initial adhesion and spreading. Biotechnol. Prog. 19 (2003) 987-999.

66 W. Wu, R.F. Giese Jr, C.J. van Oss. Linkage between ζ-potential and electron donicity of charged polar surfaces 1. Implications for the mechanism of flocculation of particle suspensions with plurivalent counterions. Colloids Surf. A Physicochem. Eng. Asp. 89 (1994) 241-252.

67 E. Watarai, R. Matsuno, T. Konno, K. Ishihara, M. Takai. QCM-D analysis of material–cell interactions targeting a single cell during initial cell attachment. Sens. Actuator B-Chem. 171 (2012) 1297-1302.

68 K.J. Verstrepen, F.M. Klis. Flocculation, adhesion and biofilm formation in yeasts. Mol. Microbiol. 60 (2006) 5-15.

69 J. Israelachvili. Differences between non-specific and bio-specific, and between equilibrium and non-equilibrium, interactions in biological systems. Q. Rev. Biophys. 38 (2005) 331-337.

70 R.M. do Nascimento, U. Sarig, N.C. da Cruz, V.R. de Carvalho, C. Eyssartier, L. Siad, J. Ganghoffer, A.C. Hernandes, R. Rahouadj. Optimized-surface wettability: A new experimental 3D modeling approach predicting favorable biomaterial–cell interactions. Adv. Theory Simul. *2*(2019), 1900079.